INTERNATIONAL JOURNAL OF REMOTE SENSING
2020, VOL. 41, NO. 12, 4549–4567
https://doi.org/10.1080/01431161.2020.1723173

Taylor & Francis
Taylor & Francis Group

Check for updates

How far can we trust forestry estimates from low-density LiDAR acquisitions? The Cutfoot Sioux experimental forest (MN, USA) case study

Enrico Borgogno Mondino[a], Vanina Fissore[a], Michael J. Falkowski[b] and Brian Palik[c]

[a]DISAFA, University of Torino, Grugliasco, Italy; [b]Department of Ecosystem Science and Sustainability, Colorado State University, Fort Collins, CO, USA; [c]Applied Forest Ecology, USDA Forest Service, Northern Research Station, Grand Rapids, MN, USA

ABSTRACT

Aerial discrete return LiDAR (Light Detection And Ranging) technology (ALS – Aerial Laser Scanner) is now widely used for forest characterization due to its high accuracy in measuring vertical and horizontal forest structure. Random and systematic errors can still occur and these affect the native point cloud, ultimately degrading ALS data accuracy, especially when adopting datasets that were not natively designed for forest applications. A detailed understanding of how uncertainty of ALS data could affect the accuracy of derivable forest metrics (e.g. tree height, stem diameter, basal area) is required, looking for eventual error biases that can be possibly modelled to improve final accuracy. In this work a low-density ALS dataset, originally acquired by the State of Minnesota (USA) for non-forestry related purposes (i.e. topographic mapping), was processed attempting to characterize forest inventory parameters for the Cutfoot Sioux Experimental Forest (north-central Minnesota, USA). Since accuracy of estimates strictly depends on the applied species-specific dendrometric models a first required step was to map tree species over the forest. A rough classification, aiming at separating conifers from broadleaf, was achieved by processing a Landsat 8 OLI *(Operational Land Imager)* scene. ALS-derived forest metrics initially greatly overestimated those measured at the ground in 230 plots. Conversely, ALS-derived tree density was greatly underestimated. To reduce ALS uncertainty, trees belonging to the dominated plane were removed from the ground dataset, assuming that they could not properly be detected by low-density ALS measures. Consequently, MAE (Mean Absolute Error) values significantly decreased to 4.0 m for tree height and to 0.19 cm for diameter estimates. Remaining discrepancies were related to a *bias* affecting the native ALS point cloud, which was modelled and removed. Final MAE values were 1.32 m for tree height, 0.08 m for diameter, 8.5 m^2 ha^{-1} for basal area, and 0.06 m for quadratic mean diameter. Specifically focusing on tree height and diameter estimates, the significance of differences between ground and ALS estimates was tested relative to the expected 'best accuracy'.

ARTICLE HISTORY
Received 18 September 2018
Accepted 4 December 2019

CONTACT Vanina Fissore vanina.fissore@yahoo.com DISAFA, University of Torino, L. go Paolo Braccini 2, Grugliasco, TO 10095, Italy

Supplemental data for this article can be accessed here.

© 2020 Informa UK Limited, trading as Taylor & Francis Group

Results showed that after correction: 94.35% of tree height differences were lower than the corresponding reference value (2.86 m); 70% of tree diameter differences were lower than the corresponding reference value (4.5 cm for conifers and 6.8 cm for broadleaf). Finally, forest parameters were computed for the whole Cutfoot Sioux Experimental Forest. Main findings include: 1) all forest estimates based on a low-density ALS point cloud can be derived at plot level and not at a tree level; 2) tree height estimates obtained by low-density ALS point clouds at the plot level are highly reasonably accurate only after testing and modelling eventual error bias; 3) diameter, basal area, and quadratic mean diameter estimates have large uncertainties, suggesting the need for a higher point density and, probably, a better mapping of tree species (if possible) than achieved with a remote sensing-based approach.

1. Introduction

Discrete return LiDAR (Light Detection And Ranging) technology from aircraft (ALS – Aerial Laser Scanner) is a proven tool for many forest applications. Due to its high accuracy in measuring vertical and horizontal forest structure, use of ALS for forest characterization has increased considerably over the last few decades. It has been successfully applied in support of operational forest inventories by deriving accurate, high resolution estimates of many forest structural properties including tree height (Morsdorf et al. 2004; Andersen, Reutebuch, and McGaughey 2006; Hopkinson et al. 2004; Edson and Wing 2011; Saremi et al. 2014; Falkowski et al. 2006, 2008), diameter (Popescu 2007; Saremi et al. 2014), canopy size (Means et al. 2000; Popescu and Zhao 2008), volume (Hinsley et al. 2002; Riaño et al. 2004; Latifi et al. 2015) and vertical distribution of tree canopy (Dubayah and Drake 2000). In traditional forest inventories, tree attributes are collected in discrete ground sample plots, which are assumed to be representative of the whole forest. Conversely, ALS data can provide information across large spatial extents, ranging from tree to landscape scales (McRoberts, Tomppo, and Næsset 2010). ALS-derived tree heights can be used to estimate forest structural parameters such as tree diameter and basal area via numerical model estimation, both for single species or mixed-species forests (e.g. tree diameter; VanderSchaaf 2012). Given this wide and increasing use, a detailed understanding of how uncertainty in the LiDAR dataset affects the uncertainty of derived forest inventory metrics, i.e. tree height, stem diameter, and basal area, is required.

A specific need is to understand if low-density LiDAR acquisitions or ALS datasets acquired for other purposes can be used in forestry applications. Many agencies have publically available low-density LiDAR acquisitions often acquired for topographic mapping. These freely available datasets may cover large geographic areas; their use in forest-related research and management is an opportunity increasingly explored. For instance, low-density LiDAR dataset have been used to estimate forest aboveground biomass in northern Italy (Montagnoli et al. 2015) and for testing tree species identification (e.g. Suratno, Seielstad, and Queen 2009).

In this work, we used a free low-density ALS dataset, acquired by the State of Minnesota (USA), together with Landsat 8 OLI (Operational Land Imager) data, to characterize forest structure of the Cutfoot Sioux Experimental Forest (CEF) located in north-central Minnesota (USA). The joint use of ALS data with multispectral satellite data was used since ALS measures

alone cannot be efficiently used to separate tree species, while multispectral satellite data, in spite of its reduced geometric resolution, can be used to map main vegetation classes (e.g. broadleaved trees versus coniferous trees) based on their spectral signatures. Determining tree species class is of paramount importance when using tree height as a predictor of other tree parameters via numerical dendrometric models.

Specifically, we investigated structural properties of forest at both tree and plot scales. At the tree-scale, we examined tree height (m) and diameter (m). At the plot-scale, we examined tree density, mean height (m), mean diameter (m), mean basal area (BA, m^2 ha^{-1}), and quadratic mean diameter (QMD, cm).

We hypothesized that 1) low-density LiDAR-derived forest estimates could be given at tree level and/or at plot level, and, 2) low-density LiDAR-derived estimates were comparable to the same measures obtained from ground-based data collection. To test these hypotheses, estimates were derived from both ground and ALS data and their consistency tested at both tree- and plot-scales. A rather weak consistency was initially found. Authors hypothesized that this not favourable situation could be due to two factors; first, a limitation of the system, as it is a 'low-density' acquisition system, and, second, a possible error *bias* affecting the native point cloud. In fact, it is known that LiDAR raw data can be affected by many random and systematic errors introduced during data acquisition (depending from flight acquisition geometry) (Coveney 2013) data processing, and depending on the nature of the surface hit by the laser pulse (e.g. land cover categories, vegetation classes, slope) (Hyyppä et al. 2005). Consequently, a further investigation was achieved and some actions, included error bias modelling, adopted to correct ALS estimates, at both tree and plot scale. We finally computed forest inventory parameters for the whole study area at the plot-scale. Measures distribution was summarized computing correspondent Empirical Cumulative Distribution Functions (ECDF).

2. Materials and methods

2.1. Study area

The study area is a portion of the Cutfoot Experimental Forest (CEF, 507 ha) located within the Chippewa National Forest in north-central Minnesota (Itasca county, USA) at 47°40´ N, 94°5´ W (Figure 1). CEF is dominated by red pine (*Pinus resinosa* Ait.) that originated after fires that occurred between 1864 and 1918 (Adams, Loughry, and Plaugher 2004). Additional tree species include jack pine (*Pinus banksiana* Lamb.) and eastern white pine (*Pinus strobus L.*), paper birch (*Betula papyrifera* Marsh.) and quaking Aspen (*Populus tremuloides* Michx.).

CEF study area was divided between 273 ha of managed forest, including commercial timber harvests and numerous silvicultural experiments (Buckman 1964; Adams, Loughry, and Plaugher 2004; Bradford and Palik 2009; D'Amato, Palik, and Kern 2010), and 234 ha of unmanaged, largely old-growth forest in the Sunken Lake Natural Area (Aakala et al. 2012; Fraver and Palik 2012).

2.2. Ground data

Ground data were collected as part of a forest-wide survey between May and August 2013 within 230 permanent forest inventory plots: 130 plots were located in the managed area

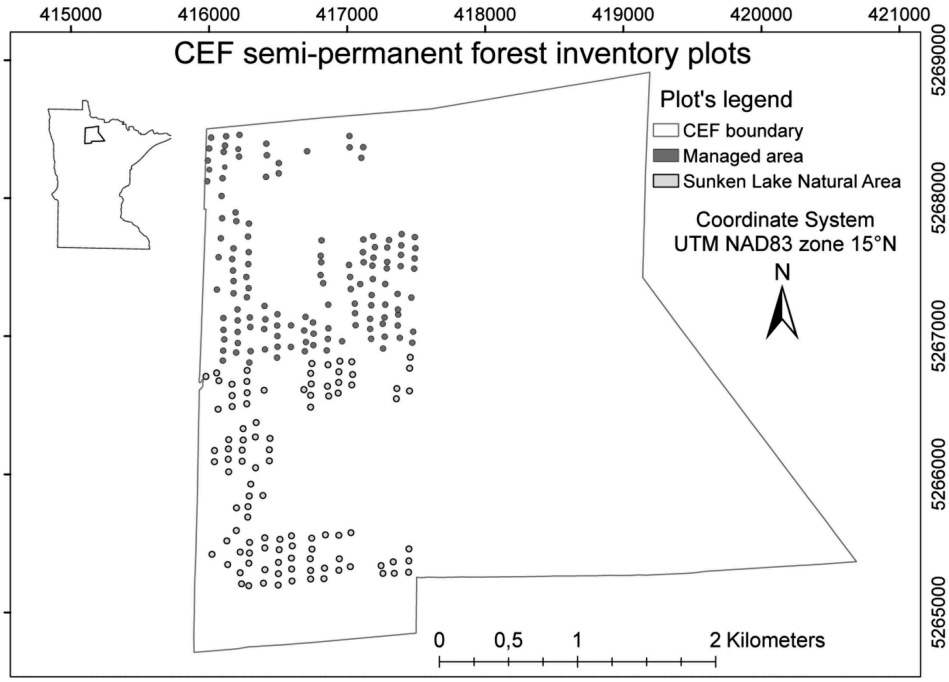

Figure 1. Map of CEF showing the distribution of surveyed plots. One hundred and thirty plots are located in the managed area (dark grey), 100 in the Sunken Lake natural area (light grey).

and 100 were located in the Sunken Lake Natural Area. There were 9851 surveyed trees, averaging about 43 trees per plot. Sampling plots had a nested design comprised three circular plots: in the outer plot, which had a radius of 16 m, tree species were identified and diameters measured for all trees ≥ 19.3-cm diameter at breast height (DBH). The central plot, which had a radius of 11.3 m, was used to tally trees ≥ 8.9 cm and < 19.3 cm DBH. Lastly, the innermost plot, which had a radius of 3.5 m, was used to tally trees with DBH < 8.9 cm and height > 0.30 m. This field sampling design is a standard approach for forest vegetation measurements in the study area. We used these ground data in our study because it was freely available and because it was collected near in time to the LiDAR data (see next section).

For the ground data, tree diameters were directly measured but other forest parameters were derived by computation using appropriate species-specific regression models calibrated from the USDA Forest Service Forest Inventory and Analysis database for northern Minnesota, USA. Single tree measures and estimations were then averaged at the plot-level to derive mean height, mean diameter, mean basal area (BA) and quadratic mean diameter (QMD) for each plot.

During ground data collection, the position of each plot centre was georeferenced by GNSS (Global Navigation Satellite System) using a GPSMAP® 60CSx, providing a position accuracy of about 10 m. Individual tree positions were measured as distance (m) and azimuth (degrees) from the plot centre. During data processing, tree positions within the plot were recovered by moving from plot centre according to distance and azimuth values.

2.3. Remotely sensed data

ALS raw data were freely obtained from the Minnesota Geospatial Information Office website (MnGeo, http://www.mngeo.state.mn.us) for the Central Lakes Region of MN. The dataset was collected over Itasca County, MN in April 2012. The data were provided in the UTM NAD83 Zone 15°N coordinate system. Vertical and horizontal accuracy values were 0.5 m and 1.15 m, respectively, at a 95% confidence level, and flight lines side overlap was 25%. ALS60, ALS70 and Optech ALTM Gemini systems were used for data acquisition. General specifications of acquisition conditions included the following: AGL (Above Ground Level) average flying height ranged between 2072.6 m and 2377.4 m; MSL (Mean Sea Level) average flying height ranged between 2712.7 m and 2766.0 m; Average Ground Speed was about 277 km h^{-1}; Field of View (FOV) was 40 degrees; LiDAR pulse rate ranged between 99 kHz and 115.3 kHz and the scan rate between 25.1 Hz and 38 Hz. Multiple returns were recorded up to five returns; intensity values were recorded @8-bit quantization. Pulse returns density was of 0.78 pulses m^{-2}. The raw point cloud was processed via LASTools (Rapidlasso GmbH) to generate gridded digital surface model (DSM) and digital terrain model (DTM) with a 1 m cell size. A canopy height model (CHM) was generated by differencing the DSM and DTM and a *local maxima* algorithm was run to map potential trees from the correspondent CHM using SAGA GIS 7.2.

A Level 2 Landsat 8 OLI multispectral image, acquired on 11 November 2013, was downloaded from the EarthExplorer distribution system (http://www.earthexplorer.usgs.gov). It was supplied already calibrated in at-the-ground reflectance. A Landsat-8 OLI image was adopted because its geometric resolution of 30 m is consistent with ground plots size (16 m radius). In this way, we assumed that each forest plot corresponded to a Landsat pixel for comparison. Moreover, since the image was multispectral, we were able to use spectral signatures of conifers and broadleaf to classify the forest.

A caveat regarding the LiDAR and ground truth data is that they were collected more than 1 year apart. However, the ground data is specifically based on measurements of trees; short of changes caused by catastrophic events (or which there were none in the study area during the period of record), there would be virtually no detectable differences in measurements taken in the spring 2012 versus summer 2013. Any difference in diameter, height, or basal area would be within the range of measurement error. Moreover, ground data were used only to directly provide diameters and trees location, and consequently the effect of the season (LiDAR: April 2012 vs Ground data: summer 2013) is inconsequential. Moreover, LiDAR acquisition for the study was collected in April, which is the beginning of a leaf-on season in the study area and the forest is conifer dominated, so the influence of differences in time of acquisition between ground and LiDAR data was minimized.

2.4. Data analysis

ALS-derived and ground measures follow opposite pathways to generate tree-level forest inventory measures. Specifically, traditional forest inventory approaches use tree diameter measurements to model tree height and other parameters, whereas ALS-based approaches use tree heights to derive diameter and other parameters. Both approaches operate through numerical models that relate diameter and height. In consistency tests of tree diameters, the LiDAR values are 'indirectly' derived by numerical modelling from

heights; when testing consistency of heights, the ground-based measures are generated by numerical approaches. Therefore, we have to preventively define some reference values (the 'best reachable accuracy') to compare uncertainty with. These can be defined while calibrating local numerical model relating diameters and height (or vice versa) by an Ordinary Least Squares (OLS) approach. A flowchart showing overall phases of analysis is available in the Supplemental material (Figure S-1).

2.4.1. Ground data processing

Using ground sampled tree diameters, we estimated by OLS the coefficients of the following numerical dendrometric model relating tree height to its diameter (Perala and Alban 1993).

$$H_s = a_s D^{b_s} + \varepsilon_s \tag{1}$$

where H_s is the estimated height for a specific species, D the ground sampled diameter, a_s and b_s are species-specific coefficients and ε_s the estimated model uncertainty.

The model was calibrated using the dataset from the USDA Forest Service Forest Inventory and Analysis database for Minnesota, downloaded from the FIA website (version 4.0, Woudenberg et al. 2010). Only the most frequently occurring species in CEF plots were considered. For the conifer class (hereinafter called 'C'): balsam fir, eastern white pine, jack pine, and red pine were included; for the broadleaf class (hereinafter called 'B'): paper birch, quaking aspen and northern red oak were included. Calibrated models were then used to compute tree heights within the surveyed plots.

The FIA data for Minnesota were chosen because the calibration of the regression models required a large amount of (freely available) reliable inventory data and, moreover, it needed to be specific for the species present in the study area, which was not obtainable from any other source.

To ensure that all diameter classes were equally represented during model calibration, OLS estimation related mean diameter and height values of predefined classes. These were defined by splitting the diameter range of variation into class widths of 2.5 cm and looking for the corresponding height values. Class diameter and height values were averaged and model parameters estimated accordingly. Standard deviation of heights belonging to the class was computed as well. The mean value of all class standard deviations ($\sigma^H{}_m$) was assumed to be the reference 'best' uncertainty to compare with ALS-derived heights. In other words, height estimations from the model were assumed to represent a class of heights having an internal variability equal to $\sigma^H{}_m$. All computations for model calibration were run through in-house appositely developed IDL (Interactive Data Language) routines.

Tree basal area (g_i) was computed according to Equation (2):

$$g_{i=} \frac{\pi}{4} \times d_i^2 \qquad (\mathrm{m}^2) \tag{2}$$

where d_i is the diameter of the i-th tree.

Estimated single tree measures were then averaged to the plot level. For each plot, mean diameter ($D^G{}_\mu$) and mean height ($H^G{}_\mu$) were computed. Plots total basal area (BA^G) was considered and computed by Equation (3), including all species in a plot:

$$BA^G = \frac{\sum_{i=1}^{n} g_i}{A_p} \qquad (m^2 ha^{-1}) \tag{3}$$

where g_i is basal area, n is the number of surveyed trees in each plot and A_p the area (ha) of the plot.

Moreover, plot mean tree density ($T^G{}_{pha}$) and plot quadratic mean diameter (QMD^G) were computed, respectively, according to Equations (4) and (5).

$$T^G{}_{pha} = \frac{n.tree}{A_p} \qquad (trees\ ha^{-1}) \tag{4}$$

$$QMD^G = \frac{BA/T_{pha}}{0.00007854} \qquad (cm) \tag{5}$$

To summarize data at plot level single tree diameters and heights were averaged within the plot.

2.4.2. Mapping tree species by satellite imagery

To map tree species, the accuracy of estimates depends on being able to apply the appropriate dendrometric model to the proper tree species. Since no a-priori knowledge of vegetation type was available, a preliminary step was needed to classify tree species before models could be applied. From an operational point of view, a species level classification of forest (tree by tree) was not possible. Nevertheless, a rough classification, aiming to separate conifers from broadleaf trees, was achieved using multispectral imagery.

For image classification, the main tree species of study area (Table 1) were analysed at the plot level; depending on the proportion of conifers and broadleaf trees, plots were labelled as 'C' if they were ≥70% coniferous species or 'B' if they were ≥70% broadleaf species. Mixed plots were excluded from the analysis. Fifty-four plots were labelled as B, 97 as C, and 79 were not considered for classification training, as they were mixed. It is worth to highlight that geometric resolution of Landsat OLI images (30 m) is consistent with plot size (16 m radius). Consequently, one can assume that each forest plot corresponds to a Landsat pixel. To collect an adequate number of training pixels each plot was used as starting point to define the corresponding Region of Interest (ROI), that was obtained by

Table 1. Dendrometric model parameters (a_s and b_s in Equation (1)) estimated by OLS for the considered tree species with reference to the US FIA database. MAE^H defines the accuracy of the estimated tree height. r is the computed Pearson's coefficient for estimated and observed measures. $\sigma^H{}_{species}$ defines the intra-species variability of tree height estimates. In the first column it is reported, for the considered species, the macro class it was assigned to (B = Broadleaf; C = Conifers). H = tree height.

Assigned class	No. trees	Species	a_s	b_s	MAE^H (m)	r	$\sigma^H{}_{species}$ (m)
C	457	Balsam fir (*Abies balsamea*)	44.926	0.758	1.19	0.99	2.38
C	792	Eastern white pine (*Pinus strobus*)	39.528	0.683	2.03	0.99	3.49
C	903	Jack pine (*Pinus banksiana*)	44.925	0.730	1.48	0.98	2.84
B	411	Northern red oak (*Quercus rubra*)	30.815	0.496	1.38	0.97	3.41
B	1830	Paper birch (*Betula papyrifera*)	31.658	0.504	1.54	0.94	3.09
B	380	Quaking aspen (*Populus tremuloides*)	36.966	0.530	1.42	0.97	3.12
C	4584	Red pine (*Pinus resinosa*)	40.005	0.737	2.05	0.98	3.27

region growing looking for similar pixels around the selected one. Any eventual relative positioning error between ground and ALS measures with respect to Landsat imagery can be ignored, as it was lower if compared with Landsat pixel size. A supervised classification (*Minimum Distance* algorithm; Richards 1999) was, therefore, run to generate the corresponding classification map, which was validated using a confusion matrix.

2.4.3. ALS data processing

The LiDAR point cloud was processed using LASTools libraries. The following operations were performed: a) point returns presenting a scanning angle greater than 15 degrees were filtered out (accuracy reduces when scanning angles are higher than 12–14 degrees over dense forest stands; Gatziolis and Andersen 2008); b) points were classified into 'ground' and 'not-ground' by LASTools "*lasground*" library (natural context parameters); c) regularization of points cloud was achieved by *las2dem* tool obtaining the correspondent DTM and DSM with a pixel size of 1 m.

A CHM of the area was generated by differencing of DSM and DTM. A specifically designed *local maxima* filter was run over CHM, to detect pixels which likely represented the top of trees.

Tree heights from ALS were extracted from CHM at the locations of the detected *local maxima*. Tree diameter was estimated by Equation (6). Model type was specifically selected and used by authors with no concern about pre-existing references from literature, but in consequence of appositely performed test involving available data.

$$D_t = e^{a_t} \times H^{b_t} + \varepsilon_t \tag{6}$$

where a_t and b_t are tree-species dependent coefficients and ε_t is the estimated model uncertainty for D_t. Differently from ground measures, ALS estimates of D_t were computed by Equation (6), differently calibrated in respect of 'C' and 'B' macro-classes. This was obtained including associated tree species according to Table 1.

To ensure that all height values were equally represented during model calibration, OLS estimation related height and diameter mean values of predefined aggregated classes from the native measures. Height classes were defined with a width of 25 cm; included measures, together with the correspondent diametric ones, were averaged at class level. The dendrometric model of Equation (6) was therefore calibrated with respect to the averaged diameter and height class values. Standard deviation of each diameter class was computed. Unlike direct dendrometric models (Equation 1), the mean of the standard deviations of class diameter was lower than the correspondent MAE^D (Mean Absolute Error, Willmott & Matsuura, 2005). MAE^D was therefore assumed to be the reference 'best' accuracy in diameter estimation from ALS data.

The forest class map from Landsat 8 imagery (FCM) was used to assign the appropriate tree class to each ALS detected tree, allowing application, at tree level, of the right dendrometric model (Equation 6).

Once height and diameter were estimated for each detected tree, T^L_{pha}, D^L_μ, H^L_μ, BA^L, and QMD^L were computed for each plot by averaging.

Using the FCM ('C' and 'B' classes), forest parameters were computed for the whole CEF study area at plot level, generating the corresponding raster maps (cell size = 30 m) of the estimates of forest parameters.

2.4.4. Ground vs ALS: testing consistency of measures

To compare measures, we first tested the consistency of tree positions as detected from ALS by the *Local Maxima* algorithm with the field surveyed positions. This comparison showed a significant displacement in positions. Consequently, a tree-to-tree comparison was unreasonable, so comparisons were made at plot level. Therefore, estimates from ALS were computed at-tree level, but comparisons with ground data were based on aggregate measures. An initial comparison of all detected trees with respect to the surveyed trees was done by computing ECDFs of T_{pha}, H_μ, D_μ, BA, and QMD for both ground and ALS measures/estimates.

Because of the importance of height measures in many forest parameter computations, and because of the trend of using ALS data for determination, a comparison was done with reference to plot average tree height values ($H^G{}_\mu$ and $H^L{}_\mu$). Uncertainty of $T^L{}_{\text{pha}}$, $D^L{}_\mu$, $H^L{}_\mu$, BA^L, and QMD^L, was measured as MAE (Equation 7).

$$\text{MAE} = \frac{1}{n}\sum_{i=1}^{n}|f_i - y_i| \tag{7}$$

where f_i is the predicted (ALS) value, y_i is the ground correspondent value and n the number of observations (n plots).

Initially, we considered that large differences could be related to the underestimation of trees number by ALS, if vegetation under the main canopy is not completely described (Reitberger et al. 2009). This in particular affected aggregated forest parameters (BA, QMD, T_{pha}) that depended on tree number. To test this hypothesis we sorted, for each plot, ground surveyed trees according to their height, selecting the tallest ones in numbers equal to those detected by ALS. We assumed that this operation removed from analysis the trees of the dominant layers that were not recorded by LiDAR, making observation distributions more similar. New ground tree height values were then calculated and compared with the ALS-derived ones. Since this comparison still showed dissimilarities, we tested if a *bias* could affect the native point cloud. For this, we compared ALS estimates with the 'filtered/reduced' ground surveyed ones. *Bias* was tested only for tree heights. We related $\Delta H_\mu = H^L{}_\mu - H^G{}_\mu$ with $H^L{}_\mu$ by scatterplot, finding a strong correlation, which was modelled to correct ALS measured tree heights both at plot and tree level. This operation proved to reduce the uncertainty of estimates.

After quantification of tree height accuracy (MAE was computed at plot level) affecting 'corrected' ALS-derived estimates, significance of both ΔH_μ and $\Delta D_\mu = D^L{}_\mu - D^G{}_\mu$ was tested. Only $|\Delta H_\mu|$ and $|\Delta D_\mu|$ higher than expected 'best' accuracy ($\sigma^H{}_m$, MAE^D respectively for tree height and diameter estimates) were assumed significant. To test this condition, the ECDFs of ΔH_μ and ΔD_μ from LIDAR from both '*biased*' and '*unbiased*' measures were computed for the whole CEF study area. These were compared to ground estimates, demonstrating that a few field surveyed measures can represent much of the forest where they were sampled.

Finally, a comprehensive description of the CEF study area using all forest parameters was developed and interpreted. A flowchart for error quantification and

modelling, and for the ECDF comparison analysis, is available in the Supplemental material (Figure S-2).

3. Results and discussions

Obtained results underlined the possibilities and limits of forest parameter estimation using low-density LiDAR point clouds in conjunction with medium resolution satellite data.

3.1. Ground data processing

The dendrometric model of Equation (1) was calibrated by OLS for the main tree species surveyed in CEF. Table 1 reports estimated coefficients and the following statistics: model MAE (tree height estimate accuracy); *r*, Pearson's correlation coefficient between observations and estimates; $\sigma^{H}_{species}$, mean standard deviation of height class for each considered tree species.

Values of Table 1 were averaged over all the species making it possible to synthesize mean accuracy expectations. The mean values were found to be 1.39 m and 2.86 m, respectively, for MAE^{H} and σ^{H}_{m}. Since the latter was the highest, it was assumed as 'best expectable accuracy' for tree height measurements. In other words, no tree height estimates from other sources are expected to be more accurate than the average intra-species variability, represented by σ^{H}_{m}.

Calibrated dendrometric models were applied to all ground surveyed trees to derive height estimates. Single trees height and diameter were then averaged over the plot and corresponding BA and QMD calculated. Moreover, at the plot-level computed forest parameters were averaged over the previously defined macro-classes ('B' = Broadleaf and 'C' = Conifers). At-class-level, average forest parameters are hereinafter indicated as: D^{G}_{μ}, H^{G}_{μ}, BA^{G}, T^{G}_{pha}, and QMD^{G} (Table 2).

3.2. ALS-based estimates

Since dendrometric models were species-specific, we proceeded to map forest vegetation by classifying a L8 OLI multispectral image. We looked for two classes: broadleaf trees and conifers. More detailed species mapping was not reliable. The training set for the Minimum Distance supervised classifier was generated by *region growing* (similarity threshold equal to 0.9) starting from the position of the surveyed 151 plot centres. A total of 591 pixels were finally selected (322 for broadleaf and 269 for conifers). Classification accuracy was 90.2%. Table 3 reports main statistics concerning Minimum Distance classification performance: Producer's and User's Class accuracy, Class Commission and Class Omission.

Once conifers and broadleaf forest areas were mapped, the inverse dendrometric models (Equation 6) specifically calibrated for both conifers 'C' and broadleaf 'B' were applied. Model parameters and MAE are reported (Table 4).

Models were applied at the single tree level (as detected by local maxima algorithm from CHM). This made it possible to compare ECDF of the forest estimates.

Table 2. Mean values of forest parameters at macro-class level ('B' = Broadleaf and 'C' = Conifers). $\overline{\sigma_H}$; $\overline{\sigma_D}$; $\overline{\sigma_{BA}}$; $\overline{\sigma_{QMD}}$ are the average values of standard deviations of plots for each computed parameter defining its intra-class average variation. T^G_{pha} =plots mean tree density; H^G_μ=plot average tree height; D^G_μ=plot average tree diameter; BA^G = Plot total basal area; QMD^G = plot quadratic mean diameter. G = ground; L = LiDAR.

			H^G_μ (m)		D^G_μ (m)		BA^G (m^2 ha^{-1})		QMD^G (cm)	
Class	No. of plots	T^G_{pha} (tree ha^{-1})	Mean	$\overline{\sigma_H}$	Mean	$\overline{\sigma_D}$	Mean	$\overline{\sigma_{BA}}$	Mean	$\overline{\sigma_{QMD}}$
'C'	97	590.73	17.0	4.34	0.30	0.11	49.35	11.71	33.34	4.27
'B'	54	414.56	16.71	4.02	0.29	0.10	34.82	10.71	33.36	4.48

Table 3. Accuracy values of classification obtained from the available Landsat 8 OLI multispectral image.

Accuracy types	Conifer	Broadleaf
Producer's class accuracy (%)	89.5	91.4
User's class accuracy (%)	99.4	100.0
Class commission (%)	0.6	0.0
Class omission (%)	10.5	7.7

Mean descriptive statistics for D^L_μ, H^L_μ, BA^L, T^L_{pha}, and QMD^L for 'C' and 'B' classes were computed (Table 5).

3.3. Ground vs ALS: testing consistency of measures

The first result from the ALS dataset was tree detection and positioning. First, we tested tree positions from LiDAR with the positions from ground survey. Consistency proved to be very poor (example available in Supplemental material–Figure S-3); this was likely related to the low accuracy GNSS receiver used during plot surveys. Additionally, only plot centres were surveyed by GNSS, while tree positions inside the plots were measured using distance (m) and azimuth (degrees) from the plot centre. These processes may have degraded the reliability of positioning. Moreover, since plot centre position was surveyed by a simple 'pseudo-range' approach (C/A code measurement), the reference point (centre of plot) is known to have an accuracy of 5–10 m, making final tree positioning at the ground potentially unreliable.

Consequently, only the analysis of plot-level aggregated measures was possible. Considering all trees falling in the sampled plots, the T_{pha} ECDFs from ground and from ALS were computed and compared (Figure 2).

Table 4. Dendrometric model parameters (for LiDAR-derived measures, from height measures to diameter estimates) separately estimated by OLS for broadleaves and conifers. MAE^D, r and $\sigma^D_{species}$ diameter estimates statistics are reported too (D = diameter). MAE^D defines the accuracy of the estimated tree diameter from LiDAR. r is the Pearson's coefficient for estimated and observed measures. $\sigma^D_{species}$ defines the intra-species variability of tree diameter estimates.

Class	a_s	b_s	MAE^D (m)	r	$\sigma^D_{species}$ (m)
'C'	−5.156	1.388	0.045	0.985	0.006
'B'	−6.957	1.983	0.068	0.960	0.006

Table 5. Mean values of forest parameters at macro-class level ('B' = Broadleaf and 'C' = Conifers) as resulting from LiDAR data. $\overline{\sigma_H}$; $\overline{\sigma_D}$; $\overline{\sigma_{BA}}$; $\overline{\sigma_{QMD}}$ are the average values of standard deviations of plots for each computed parameter defining its intra-class average variation. T^L_{pha} = plots mean tree density; H^L_μ=plot average tree height; D^L_μ=plot average tree diameter; BA^L = Plot total basal area; QMD^L = plot quadratic mean diameter.

	T^L_{pha} (tree ha^{-1})	H^L_μ (m)		D^L_μ (m)		BA^L (m^2 ha^{-1})		QMD^L (cm)	
Area		Mean	$\overline{\sigma_H}$	Mean	$\overline{\sigma_D}$	Mean	$\overline{\sigma_{BA}}$	Mean	$\overline{\sigma_{QMD}}$
'C'	246.89	24.73	2.20	0.51	0.06	53.22	19.76	52.0	6.58
'B'	216.47	22.13	2.98	0.47	0.12	43.82	24.45	48.97	10.78

Underestimation of trees number from ALS is likely related to the low density of the native point cloud, where only trees belonging to the dominant layer of forest could be detected. To better evaluate a possible effect of this phenomenon, we also computed and compared ECDFs of D_μ and H_μ (at-plot-level aggregated measures) from both ground data and LiDAR (Figure 3).

ALS proved to overestimate H_μ, with the majority of plot mean heights lower than 27 m; conversely, mean heights from ground-surveyed plots were mostly lower than 17 m. Since D_μ estimation from ALS strictly depends on measured tree heights, ECDF of D_μ was largely different for LiDAR and ground data, showing, again, a general overestimation by ALS. ECDFs of BA and QMD from ground surveys and LiDAR were also compared. Since computations directly involve diameter values and tree numbers within plots, both BA and QMD from LiDAR were overestimated (Figure 4). BA in particular shows that LiDAR is limited when recording the smallest trees (i.e. smaller diameter values) in a plot.

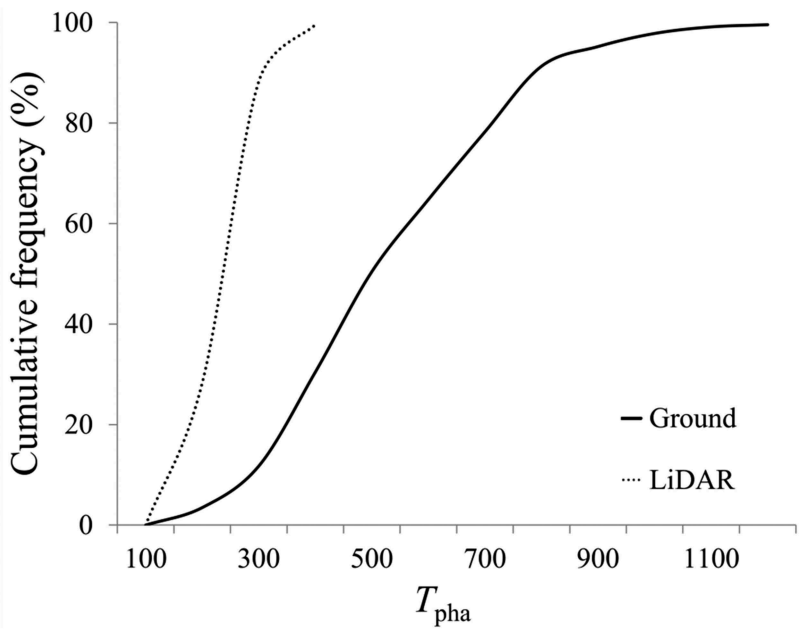

Figure 2. ECDF of ground- (solid line) and LiDAR-derived (dotted line) T_{pha}, built considering values for all assessed plot (151).

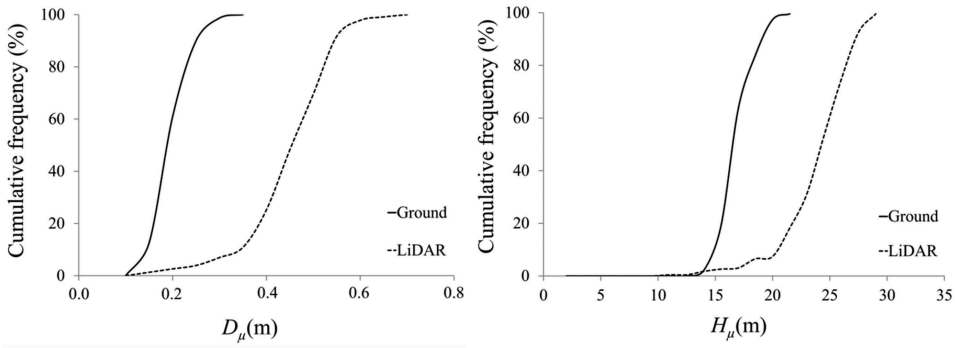

Figure 3. ECDFs. (left) plot mean tree diameter and (right) plot mean tree height from ground (solid line) and LiDAR (dotted line).

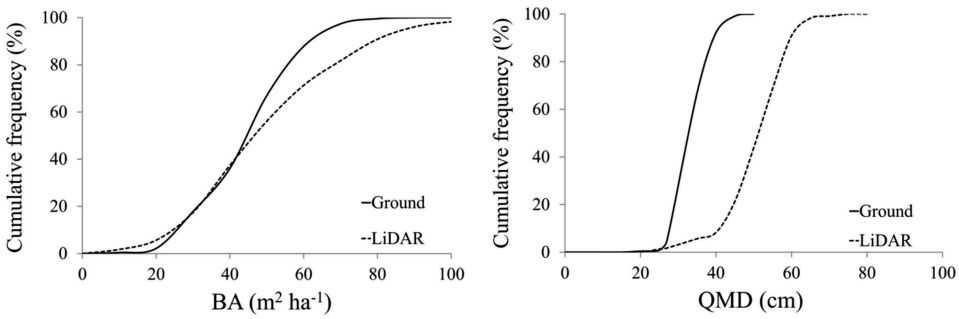

Figure 4. ECDFs. (left) BA and (right) QMD from ground (solid line) and from LiDAR (dotted line).

Overestimation of BA occurs only for larger values (i.e. of diameter) which, given the above-mentioned limitations of ALS, should be carefully considered.

Focusing on plot-level mean tree height, the difference $\Delta H_\mu = H^L{}_\mu - H^G{}_\mu$ was computed, testing its value against the expected 'best' accuracy for tree height measures, i.e. intra-plot average variation of tree heights as computed from ground observations ($\sigma^H{}_m$ = 2.86 m). We found that in 89.1% of plots, ΔH_μ exceeded $\sigma^H{}_m$. Complete statistics concerning all forest parameter estimations by ALS with respect to ground measures are reported in Table 6.

Measures at the plot level contain some apparent paradoxes, in particular, the relationship between ALS underestimation of tree number (T_{pha}) and overestimation of BA (for higher diameter values) and QMD. The interpretation key, in author's opinion, is specifically resident in the only direct measure which is expected by LiDAR, i.e. tree height. The data confirm that most of the inconsistency in estimates is related to this native error, which in our study resulted in overestimates of heights. This should alert users of low-density ALS datasets to the importance of having an appropriate number of ground observations to avoid highly distorted measures. If ground observations (surveyed plots) were available, users should use them to model *biases*, with special attention given to tree height measures from ALS.

Table 6. Percentages of plots over/under-estimating H_μ, D_μ, BA, T_{pha} and QMD from LiDAR in respect of the ground surveyed ones.

	Overestimation by LiDAR	Underestimation by LiDAR	
	Plots (%)		MAE
T_{pha} (no. trees)	3.1	96.9	294.73
H_μ (m)	96.5	3.5	7.22
D_μ (m)	97.0	3.0	0.21
BA (m^2 ha^{-1})	54.7	45.2	14.26
QMD (cm)	95.6	4.75	0.22

Observed discrepancies between LiDAR and ground measures could be related to tree density underestimation by LAS, which inevitably conditions forest parameter computations, and possible *biases* affecting native LiDAR point cloud.

We first explored tree density underestimation as a possible reason of inconsistency. To test this assumption, we forced ground plot tree density to be equal to the LiDAR derived one (according to the strategy described in Materials and Method – 3.4 *Ground vs ALS: testing consistency of measures*). This resulted in new values of $H^G{}_\mu$ and $D^G{}_\mu$ ($\hat{H}^G_\mu$and $\hat{D}^G_\mu$). Analysis was accomplished only for heights and diameters.

After reduction of ground detected trees, new MAE values were computed; 4.0 m for heights and 0.19 m for diameters.

These results proved that tree density is a factor conditioning consistency between LiDAR and ground tree parameters estimation. Once removed, residual differences suggested that some further *biases* could affect native ALS measures. Bias analysis compared ΔH_μ with $H^L{}_\mu$ by scatterplot. This had a coefficient of determination (R^2) of 0.65 (R = 0.80), supporting the hypothesis that a systematic error could affect original ALS data. A logarithmic regression (Equation 8) was used to model the existing *bias* (Figure 5).

$$\varepsilon = \Delta H_\mu = 15.37 \times \ln(H^L_\mu) - 44.98 \tag{8}$$

where ε is the correction to apply to $H^L{}_\mu$ to minimize *bias*.

The tree height *bias* model was applied at the tree level. The heights of all LAS-detected trees (H^L_t) in the CEF study area were corrected (Equation 9) and new plot height mean values $\left(\hat{H}^L_\mu\right)$ computed and compared with the ground surveyed ones (after tree number reduction).

$$\widehat{H^L_t} = H^L_t - \varepsilon \tag{9}$$

New height differences $\hat{\Delta}H_\mu = \left(\hat{H}^L_\mu - \hat{H}^G_\mu\right)$ were computed together with corresponding MAE. Statistics showed that 94.35% of heights differences, after correction, were brought within 'best accuracy' ($\sigma^H{}_m$). MAE was reduced to 1.32 m. Similarly, statistics for new diameter differences, $\hat{\Delta}D_\mu = (\hat{D}^L_\mu - \hat{D}^G_\mu)$, were calculated, showing that 70.0% of diameter differences, after correction, were brought within 'best accuracy' (MAE^D). Diameter MAE was reduced from 0.19 m down to 0.08 m, greatly improving the 'best expected accuracy' from dendrometric models.

After removing *bias* from ALS measures at the tree level, the study area was divided using a 30 m grid size graticule, computing, for each squared element, the correspondent

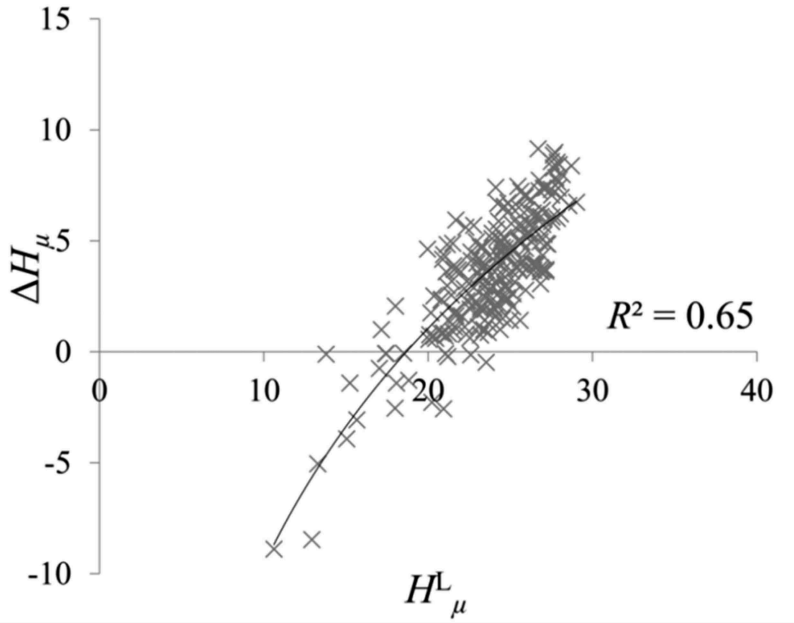

Figure 5. Bias trend modelling. The relationship linking (height difference between ground- and LiDAR-derived measures) and $H^L{}_\mu$ (plot average tree height from LiDAR) was approximated by a logarithmic regression.

height mean value ($\widehat{H'}^L_\mu$) and tree diameter mean value ($\widehat{D'}^L_\mu$) obtained by considering all trees included in the element as detected by the Local Maxima algorithm.

ECFDs of ground- and LAS-derived (de-biased) measures were computed to test: a) if consistency ALS-derived tree heights and diameters were improved at the plot level; and b) if plot statistics from the ground sampling represented the entire study area. ECFDs are reported in Figure 6.

The comparison demonstrated that, after *bias* removal and tree density correction, ECDFs of ground- and ALS-derived measures were more consistent. Specifically focusing on diameter values, residual inconsistency was probably due to limitation of the applied inverse dendrometric model that was calibrated without separating all tree species (calibration was at 'B'/"C" class level). Given the strong improvement of LiDAR estimates of tree diameters and heights at plot level after correction, new values of $\widehat{BA}^L$ and $\widehat{QMD}^L$ were recomputed from unbiased $\hat{H}^L_t$ and $\hat{D}^L_t$ for all the cells of the graticule covering the whole study area. Figure 7 shows ECDFs of the new estimated parameters.

Figure 7 demonstrates that BA and QMD estimates from ALS derived unbiased height tree measurements are more consistent with the ground surveyed data. Residual differences (MAE) for both BA and QMD estimates were 8.5 m^2 ha^{-1} and 6.0 cm, respectively.

4. Conclusions

This work presents a simple and fast method to test ALS-derived forest measures and proposes a statistically based approach to remove/minimize error *bias* that potentially affects native LiDAR point clouds. A low-density ALS point cloud and a freely available

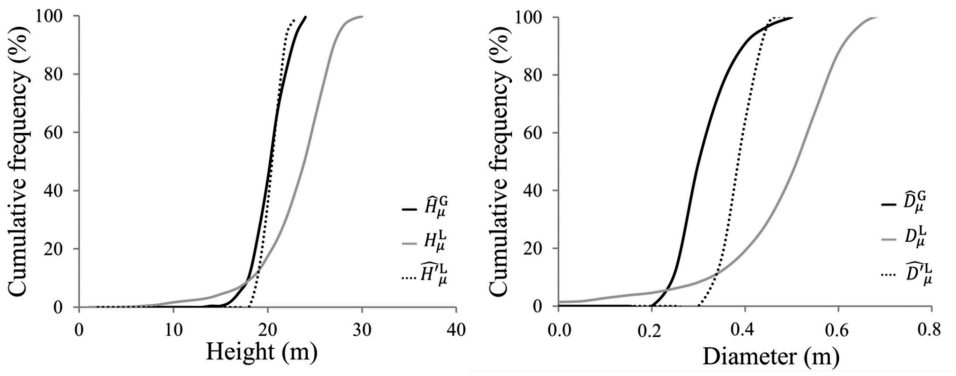

Figure 6. (left) ECDF of $\hat{H}_{\mu}^{G}$ (black solid line, ground-derived at-plot level tree height estimates after reduction), H_{μ}^{L} (grey line, LiDAR-derived at-plot level tree height estimates before bias removal) and $\widehat{H'}_{\mu}^{L}$) (dotted black line, LiDAR-derived at-plot level tree height estimates after bias removal); (right) ECDF of $\hat{D}_{\mu}^{G}$ (black solid line, ground-derived at-plot level tree diameter estimates after reduction), D_{μ}^{L} (grey line, LiDAR-derived at-plot level tree diameter estimates before bias removal) and $\widehat{D'}_{\mu}^{L}$ (dotted black line, LiDAR-derived at-plot level tree diameter estimates after bias removal). G = ground; L = LiDAR.

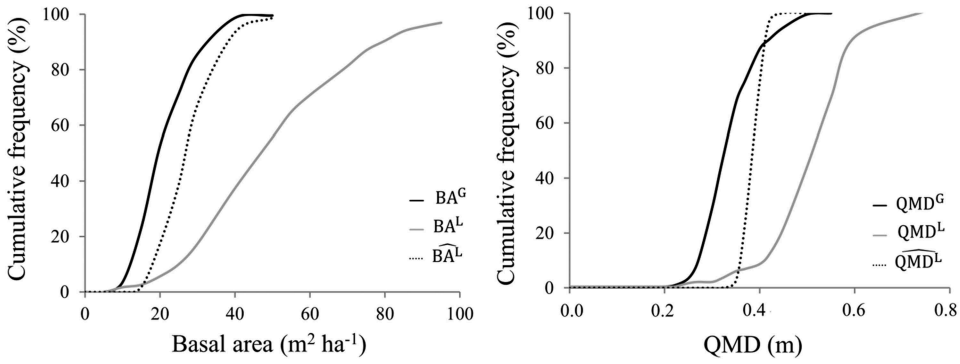

Figure 7. (left) ECDF of ground derived BA^{G} (black solid line), LiDAR-derived BA^{L} before (grey line) and $\widehat{BA}^{L}$ after (dotted black line) correction; (right) ECDF of field QMD^{G} (black solid line), LiDAR-derived QMD^{L} before (grey line) and $\widehat{QMD}^{L}$ after (dotted black line) correction. Note that ECDFs from ground estimates refer just to the plot, while ECDFs from LiDAR estimates concern all CEF (calculated at plot level considering a 30 × 30 grid cell). G = ground, L = LiDAR.

Landsat 8 OLI image were used to accomplish this task. Low density/resolution datasets are an important resource in many fields since they are often available for free and, generally, cover large geographic areas. In this work, Landsat imagery was used to classify forest cover in the Cutfoot Experimental Forest (CEF, Minnesota USA); consequently, conifers and broadleaf species were detected and mapped. This, in turn, made it possible to calibrate and apply more appropriate dendrometric models to estimate tree diameter from height when deriving forest metrics from LiDAR. Validation of estimates at tree level proved to be problematic mainly due to the great uncertainty affecting plot position from

ground measures. All comparisons were, therefore, operated at plot level (230 plots) by aggregation. Initially, uncertainty (MAE) of forest metrics estimates resulted surprisingly high and tree density was significantly underestimated by LiDAR. The joint interpretation of these two facts led authors to remove trees belonging to the dominated layers from the ground dataset, admitting that low-density ALS point cloud is not able to detect trees of the dominate layers. A significant improvement was obtained, but it was still not satisfactory. Residual errors, assumed to be related to a *bias* affecting the native LiDAR point cloud, were further minimized by statistical modelling finally reaching MAE values of 1.32 m, 0.08 m, 8.5 m^2 ha^{-1}, and 0.06.0 m for H_μ, D_μ, BA, and QMD, respectively. Significance of diameter and height errors was tested against the expected reference accuracies showing that 5.65% and 30% of errors in tree height and diameter estimates were significant (therefore measurable). The lower accuracy of diameter estimates is probably related to the adopted procedure, that applies generic dendrometric models, calibrated for wide forest classes (conifers and broadleaf) with no regard for the actual tree species. We can, therefore, conclude that low-density LiDAR point clouds can be successfully used to get tree height estimates at plot level; but this has to be done only after testing and modelling eventual error *bias* affecting native data. Conversely, diameter, basal area and QMD estimates suffer from significant uncertainty. Better estimates could result from the adoption of higher density point clouds and with a better knowledge of local tree species. At the moment, a tree-level approach is not reliable while working with low-density LiDAR point clouds, that, despite these conditions, can give a reasonable quantification of the standard forest metrics over wide areas.

Disclosure statement

No potential conflict of interest was reported by the authors.

References

Aakala, T., S. Fraver, B. J. Palik, and A. W. D'Amato. 2012. "Spatially Random Mortality in Old-growth Red Pine Forests of Northern Minnesota." *Canadian Journal of Forest Research-Review Canadian Rech. Forest* 42: 899–907.

Adams, M. B., L. Loughry, and L. Plaugher. 2004. "Experimental Forests and Ranges of the USDA Forest Service". In *USDA For. Serv. Gen. Technical Report, NE-321*, 178.

Andersen, H. E., S. E. Reutebuch, and R. J. McGaughey. 2006. "A Rigorous Assessment of Tree Height Measurements Obtained Using Airborne Lidar and Conventional Field Methods." *Canadian Journal of Remote Sensing* 32 (5): 355–366. doi:10.5589/m06-030.

Bradford, J. B., and B. J. Palik. 2009. "A Comparison of Thinning Methods in Red Pine: Consequences for Stand-level Growth and Tree Diameter." *Canadian Journal of Forest Research* 39: 489–496. doi:10.1139/X08-201.

Buckman, R. E. 1964. "Effects of Prescribed Burning on Hazel in Minnesota." *Ecology* 45: 626–629. doi:10.2307/1936114.

Coveney, S. 2013. "Association of Elevation Error with Surface Type, Vegetation Class and Data Origin in Discrete-returns Airborne LiDAR." *International Journal of Geographical Information Science* 27 (3): 467–483. doi:10.1080/13658816.2012.695794.

D'Amato, A. W., B. J. Palik, and C. C. Kern. 2010. "Growth, Yield, and Structure of Extended Rotation Pinus Resinosa Stands in Minnesota, USA." *Canadian Journal of Forest Research* 40: 1000–1010. doi:10.1139/X10-041.

Dubayah, R., and J. Drake. 2000. "LiDAR Remote Sensing for Forestry Applications." *Journal of Forestry* 98: 44–46.

Edson, C., and M. G. Wing. 2011. "Airborne Light Detection and Ranging (Lidar) for Individual Tree Stem Location, Height, and Biomass Measurements." *Remote Sensing* 3: 2494–2528. doi:10.3390/rs3112494.

Falkowski, M. J., A. M. S. Smith, A. T. Hudak, P. E. Gessler, L. A. Vierling, and N. L. Crookston. 2006. "Automated Estimation of Individual Conifer Tee Height and Crown Diameter via Two-dimensional Spatial Wavelet Analysis of Lidar Data." *Canadian Journal of Remote Sensing* 32 (2): 153–161. doi:10.5589/m06-005.

Falkowski, M. J., A. M. S. Smith, P. E. Gessler, A. T. Hudak, L. A. Vierling, and J. S. Evans. 2008. "The Influence of Conifer Forest Canopy Cover on the Accuracy of Two Individual Tree Measurement Algorithms Using Lidar Data." *Canadian Journal of Remote Sensing* 34 (2): S338–S350. doi:10.5589/m08-055.

Fraver, S., and B. J. Palik. 2012. "Stand and Cohort Structures of Old-growth Pinus Resinosa-dominated Forests of Northern Minnesota, USA." *Journal of Vegetable Science* 23: 249–259. doi:10.1111/j.1654-1103.2011.01348.x.

Gatziolis, D., and H. E. Andersen. 2008. "A Guide to LIDAR Data Acquisition and Processing for the Forests of the Pacific Northwest." In *Gen. Technical Report. PNW-GTR-768*. Portland, OR: U.S. Department of Agriculture, Forest Service, Pacific Northwest Research Station.

Hinsley, S., R. Hill, D. Gaveau, and P. Bellamy. 2002. "Quantifying Woodland Structure and Habitat Quality for Birds Using Airborne Laser Scanning." *Functional Ecology* 16 (6): 851–857. doi:10.1046/j.1365-2435.2002.00697.x.

Hopkinson, C., L. Chasmer, C. Young-Pow, and P. Treitz. 2004. "Assessing Forest Metrics with a Ground-based Scanning Lidar." *Canadian Journal of Forest Research* 34 (3): 573–583. doi:10.1139/x03-225.

Hyyppä, H., X. Yu, J. Hyyppä, H. Kaartinen, S. Kaasalainen, E. Honkavaara, and P. Rönnholm. 2005. "Factors Affecting the Quality of DTM Generation in Forested Areas." In *ISPRS Workshop "Laser scanning 2005"*. Enschede, the Netherlands.

Latifi, H., F. E. Fassnacht, J. Müller, A. Tharani, S. Dech, and M. Heurich. 2015. "Forest Inventories by LiDAR Data: A Comparison of Single Tree Segmentation and Metric-based Methods for Inventories of A Heterogeneous Temperate Forest." *International Journal of Applied Earth Observation and Geoinformation* 42: 162–174. doi:10.1016/j.jag.2015.06.008.

McRoberts, R., E. Tomppo, and E. Næsset. 2010. "Advances and Emerging Issues in National Forest Inventories." *Scandinavian Journal of Forest Research* 25 (4): 368–381. doi:10.1080/02827581.2010.496739.

Means, J., S. Acker, B. Fitt, M. Renslow, L. Emerson, and C. Hendrix. 2000. "Predicting Forest Stand Characteristics with Airborne Scanning Lidar." *Photogrammetric Engineering and Remote Sensing* 66 (11): 1367–1371.

Montagnoli, A., S. Fusco, M. Terzagni, A. Kirschbaum, D. Pflugmacher, W. B. Cohen, G. S. Scippa, and D. Chiatante. 2015. "Estimating Forest Aboveground Biomass by Low Density Lidar Data in Mixed Broadleaved Forests in the Italian Pre-Alps." *Forest Ecosystem* 2: 10. doi:10.1186/s40663-015-0035-6.

Morsdorf, F., E. Meier, B. Kötz, K. Itten, M. Dobbertin, and B. Allgöwer. 2004. "Lidar-based Geometric Reconstruction of Boreal Type Forest Stands at Single Tree Level for Forest and Wildland Fire Management." *Remote Sensing of Environment* 92 (3): 353–362. doi:10.1016/j.rse.2004.05.013.

Perala, D. A., and D. H. Alban. 1993. "Allometric Biomass Estimators for Aspen-biased Ecosystems in the Upper Great Lakes." In *Res. Pap. NC-314*, 38. St. Paul, MN: U.S. Department of Agriculture, Forest Service, North Central Forest Experiment Station.

Popescu, S. C. 2007. "Estimating Biomass of Individual Pine Trees Using Airborne Lidar." *Biomass and Bioenergy* 31 (9): 646–655. doi:10.1016/j.biombioe.2007.06.022.

Popescu, S. C., and K. Zhao. 2008. "A Voxel-based Lidar Method for Estimating Crown Base Height for Deciduous and Pine Trees." *Remote Sensing of Environment* 112 (3): 767–781. doi:10.1016/j.rse.2007.06.011.

Reitberger, J., C. Schnörr, P. Krzystek, and U. Stilla. 2009. "3D Segmentation of Single Trees Exploiting Full Waveform LIDAR Data." *ISPRS Journal of Photogrammetry and Remote Sensing* 64: 561–574. doi:10.1016/j.isprsjprs.2009.04.002.

Riaño, D., F. Valladares, S. Condés, and E. Chuvieco. 2004. "Estimation of Leaf Area Index and Covered Ground from Airborne Laser Scanner (Lidar) in Two Contrasting Forests." *Agricultural and Forest Meteorology* 124 (3–4): 269–275. doi:10.1016/j.agrformet.2004.02.005.

Richards, J. A. 1999. *Remote Sensing Digital Image Analysis*, 240. Berlin: Springer-Verlag.

Saremi, H., L. Kumar, C. Stone, G. Melville, and R. Turner. 2014. "Sub-compartment Variation in Tree Height, Stem Diameter and Stocking in a Pinus Radiata D." *Don Plantation Examined Using Airborne LiDAR Data. Remote Sensing* 6 (8): 7592–7609.

Suratno, A., C. Seielstad, and L. Queen. 2009. "Tree Species Identification in Mixed Coniferous Forest Using Airborne Laser Scanning." *Journal of Photogrammetry and Remote Sensing* 64: 683–693. doi:10.1016/j.isprsjprs.2009.07.001.

VanderSchaaf, C. L. 2012. "Mixed-Effects Height-Diameter Models for Commercially and Ecologically Important Conifers in Minnesota." *Northern Journal of Applied Forestry* 29 (1): 15–20. doi:10.5849/njaf.11-005.

Willmott, C., and K. Matsuura. 2005. "Advantages of the Mean Absolute Error (MAE) over the Root Mean Square Error (RMSE) in Assessing Average Model Performance." *Climate Research* 30 (1): 79. doi: 10.3354/cr030079.

Woudenberg, S. W., B. L. Conkling, B. M. O'Connell, E. B. Lapoint, J. A. Turner, and K. L. Waddell. 2010. "The Forest Inventory and Analysis Database: Database Description and User's Manual Version 4.0 For Phase 2.." In *US For. Serv. Gen. Technical Report RMRS-GTR-245*.